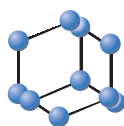


RESEARCH ARTICLE

BENTHAM
SCIENCE

Anti-Tumor Efficacy of Pyrvinium Pamoate Nanoliposomes in an Experimental Model of Melanoma



Mahdi Hatamipour¹, Mahmoud R. Jaafari^{1,2}, Mahtab Zangui^{3,4}, Neda Shakour⁵ and Amirhossein Sahebkar^{6,7,8,9,*}

¹Nanotechnology Research Center, Pharmaceutical Technology Institute, Mashhad University of Medical Sciences, Mashhad, Iran;

²Biotechnology Research Center, Pharmaceutical Technology Institute, Mashhad University of Medical Sciences, Mashhad, Iran;

³Faculty of Medicine, Mashhad University of Medical Sciences, Mashhad, Iran; ⁴Division of Hematology/Oncology, Tisch Cancer Institute, Icahn School of Medicine at Mount Sinai, New York, NY, USA; ⁵Department of Medicinal Chemistry, School of Pharmacy, Mashhad University of Medical Sciences, Mashhad, Iran; ⁶Biotechnology Research Center, Pharmaceutical Technology Institute, Mashhad University of Medical Sciences, Mashhad 9177948564, Iran; ⁷Applied Biomedical Research Center, Mashhad University of Medical Sciences, Mashhad, Iran; ⁸Polish Mother's Memorial Hospital Research Institute (PMMHRI), Lodz, Poland; ⁹School of Pharmacy, Mashhad University of Medical Sciences, Mashhad, Iran

Abstract: Background: Pyrvinium Pamoate (PP) is an old drug approved by the FDA for the treatment of pinworm infections. Recently, it has been introduced as an anti-tumor agent, however, low aqueous solubility severely limits its potential effects. In this study, we developed a liposomal formulation of pyrvinium pamoate to investigate its *in vitro* cytotoxicity and *in vivo* efficacy against melanoma cells.

ARTICLE HISTORY

Received: August 15, 2020
Revised: December 17, 2020
Accepted: January 04, 2021

DOI:
10.2174/1871520621666210217095627



Materials & Methods: As drug carriers, liposomes were fabricated using the thin-film method. PP was encapsulated within the liposomes using a remote loading method. We evaluated the morphology, particle size, and Zeta potential of the liposomes. Additionally, High-Performance Liquid Chromatography (HPLC) was employed for qualitative and quantitative analysis. Then we investigated our liposomal PP for its *in vitro* cytotoxicity as well as the tumor growth inhibition in C57BL/6 mice bearing B16F0 melanoma tumors.

Results: Based on the analytical result, the liposomal drug delivery system is a homogeneous and stable colloidal suspension of PP particles. The images of Atomic force microscopy and particle size data showed that all the prepared nanocarriers were spherical with a diameter of approximately 101 nm. According to both *in vitro* and *in vivo* studies, nanoliposomal PP exhibited an improved anti-proliferative potential against B16F10 melanoma tumor compared to free PP.

Conclusion: Liposomal encapsulation improves the water solubility of PP and enhances its anti-cancer activity.

Keywords: Pyrvinium, cancer, nanotechnology, drug delivery, melanoma, nanoliposomes.

1. INTRODUCTION

Repurposing of non-cancer medications for cancer treatment is a rapidly expanding field in oncology research. When new anti-cancer potentials are proposed for an already existing drug, because of its well-defined kinetic, dynamic, and safety profiles, it can be introduced into the clinic more rapidly than novel anti-cancer agents. Within this context, Pyrvinium Pamoate (PP) is an FDA-approved anthelmintic drug, which has been used against a variety of parasitic infections for more than fifty years. In recent years, various studies have reported its significant anti-tumor effects. According to the literature, PP treatment significantly delays growth and reduces the proliferation of cancer cells in leukemia, melanoma, breast, urothelial, colorectal, pancreas, and lung cancer [1-6]. It has also been shown to significantly inhibit colony formation, cell viability, proliferation and autophagy, migration and invasion capacity, and it also induces apoptosis in malignant cells [6, 7].

Recently, more studies have been carried out on PP to elucidate its anti-cancer mechanism of action; experimental results have

confirmed that it exerts anti-cancer effects through multiple pathways. One of its interesting mechanisms of action is the inhibition of mitochondrial oxidative phosphorylation [8]. On the other hand, in a hypoxic condition, which is more similar to cancer microenvironment, it inhibits NADH-Fumarate reductase, an important enzyme for anaerobic metabolism [9], approved by FDA for its anthelmintic properties and therapeutic function against animal-like protists, such as *Cryptosporidium parvum* and *Plasmodium falciparum*, in the 1950s. In the last 10 years, several studies have shown the novel activity of pyrvinium in tumor therapy. Some investigations have indicated that pyrvinium could delay or inhibit tumor cell proliferation in cancer models, including colon, breast, and lungs.

Wnt/ β -catenin pathway is another recognized target of PP, which plays a critical role in malignant proliferation and is now considered as an attractive cancer therapeutic target. It has been reported, at least in some cancers that it suppresses Wnt/ β -catenin pathway at multiple levels [2, 6, 10, 11]. Moreover, PI3K/AKT/mTOR is another key pathway aberrantly activated in malignant cells, the suppression of which can be achieved through PP treatment [12, 13].

One of the most interesting findings of PP is its potential against cancer stem cells [6, 14, 15]. It has been evaluated in 8 different tumor types (breast, ovarian, prostate, lung, pancreatic, me-

*Address correspondence to this author at the Department of Medical Biotechnology, School of Medicine, Mashhad University of Medical Sciences, Mashhad, Iran; Tel: 985118002288; Fax: 985118002287; E-mail: sahebkar@mums.ac.ir; amir_saheb2000@yahoo.com

lanoma, and glioblastoma); It has also been reported to successfully inhibit tumor-sphere forming ability in all 10 tested cell lines within nanomolar ranges [8]. However, despite all these potential capacities, the systemic application of PP is encountering serious limitations, and in order to advance this drug into the clinic, it likely requires some modifications.

Although, PP has shown a good safety profile even in doses as high as 35 mg/kg, when administered orally, it has very low bioavailability and is not absorbed to a clinically significant level [16]. In a clinical study, a single oral dose with 250 mg, in healthy volunteers resulted in a maximum value of 7.4 ng/ml (12.9 nM) in plasma [16]. Here, in order to improve its pharmacokinetic profile, we aimed to develop a novel delivery strategy and then investigated its efficacy both *in vitro* and *in vivo* on an experimental model of melanoma.

2. MATERIALS AND METHODS

Pyrvinium pamoate was purchased from Shanghai Boylechem (Shanghai, China). Hydrogenated Soy Phosphatidylcholine (HSPC) and 1,2-distearoyl-sn-glycero-3-phosphoethanolamine-N-[methoxy (polyethylene glycol)-2000] (PEG-DSPE2k) were purchased from Lipoid (Alabaster, Alabama, USA). RPMI 1640 and cholesterol culture medium were purchased from Sigma-Aldrich (St. Louis, MO); and MTT [3-(4,5-dimethylthiazol-2-yl)-2, diphenyltetrazolium bromide was obtained from Promega (Madison, WI). All other solvents and reagents were used as a chemical grade. Commercially available PEGylated liposomal doxorubicin (Doxil[®]) was purchased from Behestan Darou Company (Tehran, Iran).

2.1. Preparation of Liposomes

A mixture of HSPC, cholesterol, and PEG DSPE (55, 40, 5-mole ratio) was dissolved in chloroform. The solvent was removed under vacuum, generated by a rotary evaporator vacuum pump (Heidolph, Schwabach, Germany), and subsequently lyophilized by a freeze dryer. A thin film was generated and hydrated with the preheated ammonium sulfate (250 mM) solution at 65°C. Large Unilamellar Vesicles (LUV) were formed by the extrusion, done 11 times, through polycarbonate filters (100 to 400 nm pore size), using an extruder device (Burnaby, BC, Canada).

2.2. Generation of the Ion Gradient and Drug Loading

The remote loading method was used to encapsulate PP into the liposomes. The external solution (ammonium sulfate) of liposomes was exchanged into isotonic buffer solution (10 mM HEPES, 10% sucrose, pH 8.5) using a dialysis tube (12 - 14 kD). Subsequently, an acidic DMSO solution containing PP (15mg/ml) was added (50µl) to the empty liposomal dispersion. The drug entrapment process was performed at 65°C for 1 hr. The residual unloaded drug was removed through the dialyzation against 10 mM histidine 5% dextrose (pH 6.5).

2.3. Characterization of Liposomal Pyrvinium Pamoate

The particle profile size, surface charge, and surface morphology of nanoparticles were characterized. The particle size distribution and *zeta* potential of liposomal suspension were analyzed by differential light scattering technique (Malvern Instruments Ltd, Malvern, UK). A small droplet of the liposomal solution was placed on a glass slide and dried under a nitrogen stream. The surface morphology of the prepared sample was evaluated with an Atomic Force Microscopy (AFM) instrument (JPK-NanoWizard II; Berlin, Germany).

2.4. Determination of Pyrvinium Pamoate

The concentration of PP in the liposomes was determined by a fluorometric method at $\lambda_{ex} = 477$ nm and $\lambda_{em} = 579$ nm. The PP solutions at different concentrations were prepared in acidic DMSO. The emissions of samples with a spectrofluorometer (Perkin Elmer ls 45, Waltham, Massachusetts, United States) were obtained, and the calibration curve was plotted. The PP content of the liposomes was calculated using the standard calibration curve.

2.5. *In Vitro* Drug Release Study of Pyrvinium Pamoate Loaded Liposome Nanoparticles

The *in vitro* drug release profile was evaluated from a dialysis membrane (12 - 14 kDa) containing liposomal PP at pH 7.4 in Phosphate-Buffered Saline (PBS). 1 ml of the liposomal solution containing PP was added into the dialysis tube, and the outer part was filled with 200 ml of PBS (pH 7.4). The dialysis devices were gently stirred (100 r.p.m at 37°C) during release evaluation by a magnetic stirrer. At intervals of predesignated time (3, 6, 9, 12, 24, 36 and 48h), 1 ml of outer media was withdrawn and replaced with 1 ml of fresh PBS. In the obtained sample, the concentration of PP was determined by the Spectrofluorometric method.

2.6. *In Vitro* Cytotoxicity Assay

The MTT assay was performed on the melanoma cancer cell lines (B16-F10) to assess the inhibitory properties of liposomes containing PP on cell proliferation and cell viability. After incubating cell lines with drug and MTT, the absorbance of purple formazan solution was measured using a plate reader (BioTek, Synergy 2 plate reader, VT, USA). In this work, the B16-F10 cells were cultured to a 96-well plate and treated with liposomal PP in the range of 0.005 to 30 µM. 48 hours after exposure, the MTT process was stopped, and growth retardation was calculated and compared to those in the PBS group. In this study, all experiments were carried out in triplicates and were repeated twice for statistical analysis; The results are shown as the mean ± S.D.

2.7. Cell Culture

The mouse melanoma cell (B16-F10) was cultured and maintained in Dulbecco's Modified Eagle's Medium (DMEM) supplemented with 10% (v/v) FCS, 2 mM L-glutamine, 100 IU/mL penicillin and 100 mg/mL streptomycin and the cells were incubated at 37°C in a humidified incubator with a 5% CO₂ atmosphere.

2.8. Animals

Female C57BL/6 mice (4 - 6 weeks old) were housed in cages (5 animals/cage). For therapeutic tumor experiments, A total of 3×10^5 melanoma cells were injected subcutaneously into the flank of the mice and randomly distributed into 4 groups, including 1) PBS, 2) commercial liposomal doxorubicin (15mg/kg), single-dose, intravenous, 3) liposomal PP (1mg/kg/ twice a week) intravenous for 4 weeks and 4) free PP (1mg/kg/twice a week for 4 weeks). Body weight variation was recorded, and the tumor size was measured with the digital calipers during the study. The tumor volume was calculated using the modified ellipsoid formula: volume (mm³) = (length × width²)/2. The study protocol was approved by the institutional review board and the ethics committee of the Mashhad University of Medical Sciences (Mashhad, Iran) in accordance with the Animals (Scientific Procedures) Act 1986 Amendment Regulations (SI 2012/3039).

2.9. Statistical Analysis

Statistical analyses were carried out using Prism 8 (Graph Pad Prism Software, version 8, San Diego, CA). Tumor growth curves

were analysed by one-way ANOVA, followed by Tukey's *post-hoc* test. Survival curves were plotted using the Kaplan-Meier technique and analysed using the log-rank test. *P*-values of < 0.05 were considered to be statistically significant.

3. RESULTS

3.1. Fabrication of Pyrvinium Pamoate Loaded Liposome Nanoparticles

Pyrvinium was accumulated into liposomes composed of HSPC, DSPE-peg (2000) and cholesterol (% molar 55/5/40). Lipid components present in the liposomes were selected based on their physico-chemical stability, high phase-transition temperature, and the ability to provide long terminal elimination half-life. Effective drug entrapment was performed using a strong ammonium sulfate to drive the generation of an ion gradient. The drug was loaded into the aqueous liposome core using the formation of ammonium sulfate ion gradient across the liposome membrane.

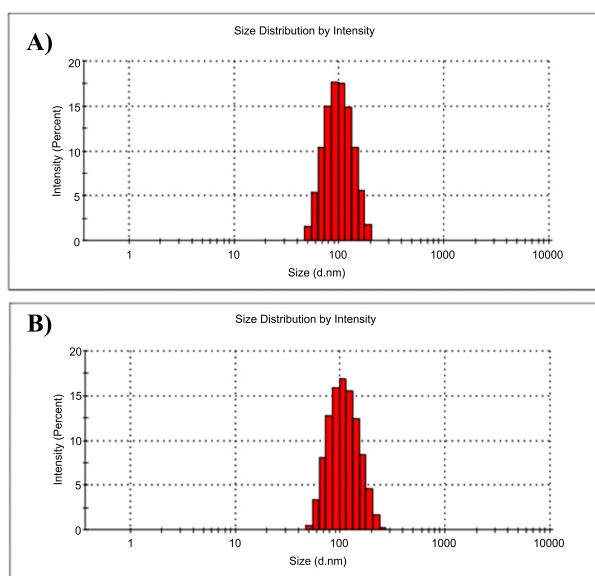


Fig. (1). The particle size analysis of empty liposomes (A) and liposomal pyrvinium pamoate (B); No significant difference was observed between the two preparations. (A higher resolution / colour version of this figure is available in the electronic copy of the article).

Table 1. Characteristics of pyrvinium pamoate nanoliposomes

| Formulation | Size (nm) | PDI | Zeta potential (mV) |
|----------------|--------------|--------------|---------------------|
| Liposomal PP | 101.6 ± 0.53 | 0.16 ± 0.01 | -11 |
| Empty liposome | 98.8 ± 0.15 | 0.069 ± 0.01 | -9.6 |

3.2. Dynamic Light Scattering Experiments

After liposomal synthesis and drug encapsulation, the size of empty liposome and liposome containing PP was determined using a light scattering instrument. The results of this examination are summarized in Fig. (1A, B) and Table 1. The result showed that the mean diameter and Polydispersity Index (PDI) of empty liposome and drug-loaded liposomes were 98.8 ± 0.15 and 101.6 ± 0.53 nm and 0.069 ± 0.01 , 0.16 ± 0.01 , respectively (Fig. 1 and Table 1). These values demonstrate that the sizes are consistent. The zeta potential analysis showed that the surface charge of the empty liposome and liposomal PP were -9.6 and -11 mV, respectively.

3.3. Surface Morphology of Liposome Nanoparticles

The AFM images (Fig. 2) show that liposomes appear to be spherically shaped, as confirmed by the DLS data.

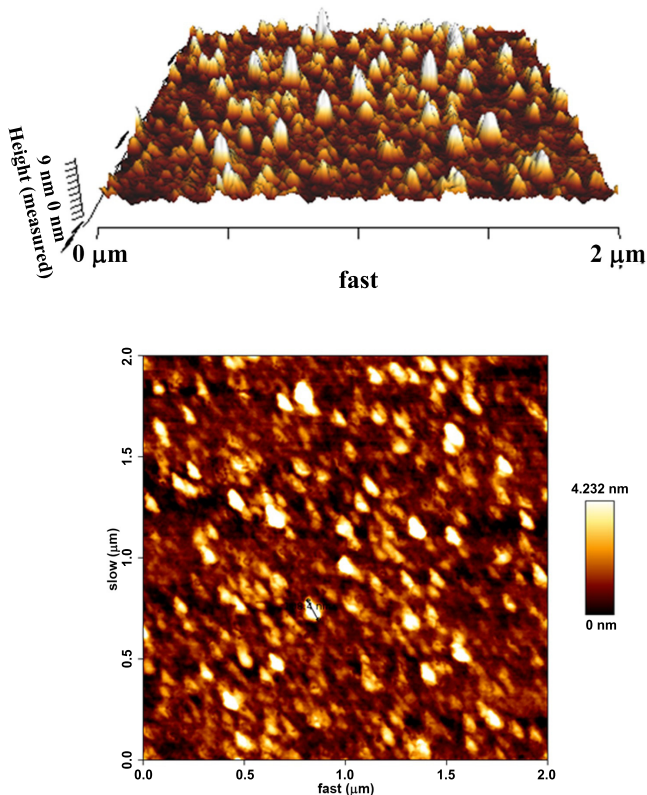


Fig. (2). AFM image of liposomal pyrvinium pamoate. (A higher resolution / colour version of this figure is available in the electronic copy of the article).

3.4. Encapsulation Efficacy

The calculated encapsulation efficacy values showed that greater than 98% of the added PP was entrapped into the liposomes within 1h at 65°C.

3.5. In Vitro Drug Release Studies

The *in vitro* drug release profile for the remotely loaded liposomal PP found that the release rate was very slow for a long time at pH 7.4 (Fig. 3).

3.6. Cell Viability

Several attempts have been made to investigate the anti-cancer effects of PP and they have shown that pyrvinium significantly inhibited the development of cancers, including colon and melanoma [2, 13, 17-19]. By considering these cases, growth-inhibitory effects of pyrvinium pamoate were evaluated on cell viability of melanoma (B16-F0) cell lines. Carefully examination of the data revealed that both liposomal and free pyrvinium pamoate at various concentrations of drug (3 - 8 μmol/L) could significantly reduce the cell viability of B16-F0 cells lines compared to the medium with only PBS in a dose-dependent manner during 48h exposure (Fig. 4A, B). The results showed that liposomal and free PP could exert cytotoxic effects with IC_{50} values of 8.3 and 3.2 μM, respectively.

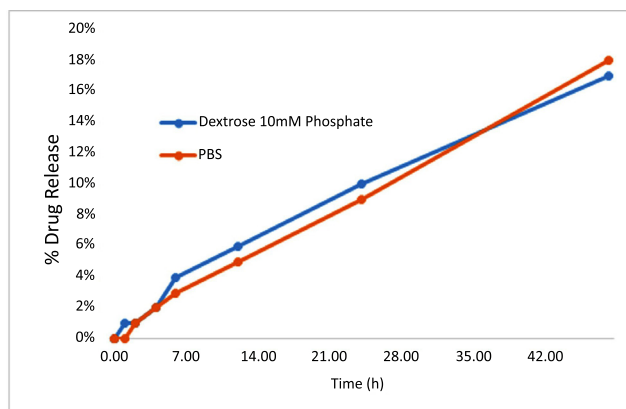


Fig. (3). *In-vitro* release profile of liposomal pyrvinium pamoate; No significant difference was observed between the release profiles in the tested media. (A higher resolution / colour version of this figure is available in the electronic copy of the article).

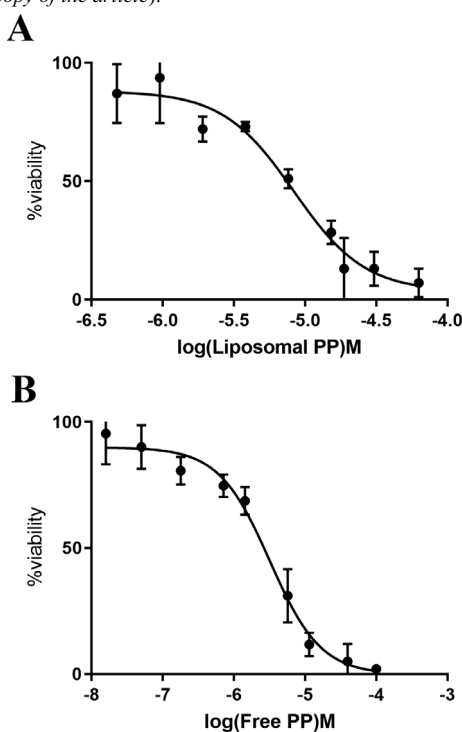


Fig. (4). Dose-response curves show % viability of B16-F0 cells treated by liposomal (A) and free (B) Pyrvinium Pamoate. (A higher resolution / colour version of this figure is available in the electronic copy of the article).

3.7. *In Vivo* Anti-tumor Effect of Injectable Liposomal PP in B16-F0 Melanoma-bearing Mice

Therapeutic efficacy of liposomal PP and free PP was assessed following intravenous administration in B16-F0 melanoma-bearing mice. The mean tumor volume (mm³) was plotted against time and illustrated in Fig. (5A). A snapshot of Kaplan-Meier analysis curves is presented in Fig. 5B; Median Survival Time (MST), TTE and %TGD are summarized in Table 2. The result of tumor growth curves and animal survivals illustrated that liposomal PP and liposomal doxorubicin were effective in inhibiting tumor growth compared to PBS ($p < 0.02$). The obtained results showed that TTE values of melanoma-bearing mice treated by liposomal PP, free PP,

Doxil, and PBS were 23 ± 1.8 , 19 ± 2.3 , 25 ± 2.1 , and 17 ± 3.3 days (Table 2), respectively. The TGD values of mice obtaining liposomal PP, free PP, and Doxil were directly compared with the PBS group, and the experimental results revealed that tumor growth rates were significantly reduced by 35.2, 11.7 and 47%, respectively (Table 2). The MST values of mice treated with liposomal PP, free PP, Doxil, and PBS groups were 23, 20, 25 and 14 days, respectively (Table 2). In comparison with PBS mice, the ILS values of mice treated with liposomal PP, free PP and Doxil were 64, 46 and 78%, respectively.

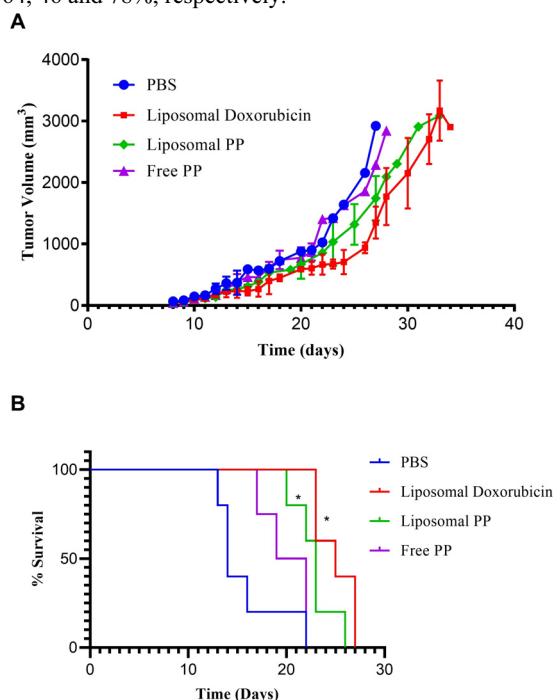


Fig. (5). *In vivo* anti-cancer effect of the formulation after a single injection in C57BL/6 mice bearing B16-F0; (A) Tumor volume (mm³) of B16-F0 melanoma was measured every 3 days. All values are reported as the mean \pm SD (n = 5 per group). (B) Kaplan-Meier curves exhibit the survival rate of treatment and control groups. * reveals that the difference between the control group with liposomal PP and Doxil groups was statistically significant ($p < 0.004$). (A higher resolution / colour version of this figure is available in the electronic copy of the article).

Table 2. Therapeutic efficacy data of different treatments in C57BL/6 mice bearing B16-F0 melanoma.

| Group | TTE (days \pm SD) | TGD (days) | MST (days) | ILS (%) |
|--------------|---------------------|------------|------------|---------|
| Control | 17 ± 3.3 | - | 14 | - |
| Liposomal PP | 23 ± 1.8 | 35.2 | 23 | 64 |
| Free PP | 19 ± 2.3 | 11.7 | 20 | 46 |
| Doxil | 25 ± 2.1 | 47 | 25 | 78 |

4. DISCUSSION

Poor solubility of PP decreases absorption across the gastrointestinal tract and, consequently, the pharmacological activity of this drug [20]. For overcoming the formulation challenges of hydrophobic drugs, nanocarriers, especially nanoliposomes, are appropriate tools. The main limitation in the widespread use of liposomal formulations is the physical and chemical instability [21, 22]. However, high chemical stability and transition temperature lipids can minimize drug leakage and enhance liposomal stability [23, 24]. Liposomes with high transition temperature lipids, such as phosphatidylcholine can provide highly stable liposomal carriers for drugs with

low solubility [23, 24]. Another convenient and frequently used strategy to enhance liposomal stability *in vivo* is PEGylation, which prevents binding to plasma proteins and reduces the rate of blood clearance by both glomerular filtration and Reticuloendothelial System (RES), therefore, lasting longer in circulation [24, 25]. Accordingly, we developed a novel and stable liposomal nano-drug carrier containing HSPC / cholesterol / DSPE-PEG, which served as a liposomal carrier for low soluble PP.

In addition to stability, a perfect drug delivery system should have a high drug-loading capacity. Although, classical liposome encapsulating, such as passive loading, cannot provide maximum drug encapsulation, active “remote” drug loading methods can increase intraliposomal hydrophobic drug concentrations [21, 22]. Lipophilic drugs are mostly encapsulated into the lipid bilayer of the liposomes. However, intraliposomal drug encapsulation into the aqueous space of the liposome enhances the stability of a drug. Here, we were able to prepare a stable PEGylated-liposome and remotely load PP into the hydrophilic core *via* the generation of ammonium sulfate ion gradient.

Quantitative analysis indicated that, using remote loading, hydrophobic PP was entrapped in the inner aqueous core with high efficiency (95%). Size distribution analysis is a key indicator of stability and uniformity. We observed that our PP-encapsulated liposomes were around 101 nm with high uniformity in the size distribution (PDI \approx 0.1). Here, we observed that PEGylated-liposomal PP exerted cytotoxic effects against B16-F0 melanoma cells with an IC₅₀ of 8.3 μ M. Previous reports have also shown a relatively wide range of IC₅₀ within 0.1 - 10 μ M for PP suppressing malignant cells of colon, breast, myeloma, and pancreas cancer [26-28]. The difference in the observed behavior between *in vitro* and *in vivo* experiments can be attributed to the barrier function of PEGylated liposomes that reduces *in vitro* cellular uptake of liposomal PP. However, PEGylation enhanced the *in vivo* pharmacokinetics of PP and increased the anti-tumor activity by protecting it against degradation and passive drug targeting through Enhanced Permeability and Retention (EPR) effect in the tumor [24, 25]. Notably, our PEGylated-liposomal PP demonstrated a marked improvement in *in vivo* effects compared to free PP with significantly higher TTE, TGD%, as well as increased survival and lifespan in treated mice (Fig. 5 and Table 2).

CONCLUSION

In summary, this novel study shows that, using PEGylated liposomes containing HSPC lipid, we can efficiently load poorly water-soluble PP by using drug-remote loading, and this significantly enhances *in vivo* anti-tumor activity of PP against melanoma. The promising results of our study, overcoming one of the main barriers for clinical application of PP, highlights its potential applicability and calls for further investigations for the exploration of the inhibitory effects of liposomal PP on other cancer models, especially metastatic and drug-resistant ones.

ETHICS APPROVAL AND CONSENT TO PARTICIPATE

The study protocol was approved by the Institutional Review Board and the Ethics Committee of the Mashhad University of Medical Sciences (Mashhad, Iran) (SI 2012/3039).

HUMAN AND ANIMAL RIGHTS

No humans were used in this study. All animals' research procedures were in accordance with the Animals (Scientific Procedures) Act 1986 Amendment Regulations.

CONSENT FOR PUBLICATION

Not applicable.

AVAILABILITY OF DATA AND MATERIALS

Not applicable.

FUNDING

This project was financially supported by the Mashhad University of Medical Sciences Research Council (Mashhad, Iran). Th by a grant from cancer research center of cancer institute of Iran (Shams cancer charity, Grant No: 37312-202-01-97) and a Grant No. 960206 of the Biotechnology Development Council of the Islamic Republic of Iran.

CONFLICT OF INTEREST

The authors declare no conflict of interest, financial or otherwise.

ACKNOWLEDGEMENTS

Declared none.

REFERENCES

- Zhang, J.; Jin, Y.; Pan, J. Inhibitory effect of the anthelmintic drug pyrvinium pamoate on T3151 BCR-ABL-positive CML cells. *Mol. Med. Rep.*, **2017**, *16*(6), 9217-9223. <http://dx.doi.org/10.3892/mmr.2017.7685> PMID: 28990077
- Zheng, L.; Liu, Y.; Pan, J. Inhibitory effect of pyrvinium pamoate on uveal melanoma cells involves blocking of Wnt/ β -catenin pathway. *Acta Biochim. Biophys. Sin. (Shanghai)*, **2017**, *49*(10), 890-898. <http://dx.doi.org/10.1093/abbs/gmx089> PMID: 28981601
- Xu, L.; Zhang, L.; Hu, C.; Liang, S.; Fei, X.; Yan, N.; Zhang, Y.; Zhang, F. WNT pathway inhibitor pyrvinium pamoate inhibits the self-renewal and metastasis of breast cancer stem cells. *Int. J. Oncol.*, **2016**, *48*(3), 1175-1186. <http://dx.doi.org/10.3892/ijo.2016.3337> PMID: 26781188
- Guo, J.; Lv, J.; Chang, S.; Chen, Z.; Lu, W.; Xu, C.; Liu, M.; Pang, X. Inhibiting cytoplasmic accumulation of HuR synergizes genotoxic agents in urothelial carcinoma of the bladder. *Oncotarget*, **2016**, *7*(29), 45249-45262. <http://dx.doi.org/10.18632/oncotarget.9932> PMID: 27303922
- Zhang, X.; Lou, Y.; Zheng, X.; Wang, H.; Sun, J.; Dong, Q.; Han, B. Wnt blockers inhibit the proliferation of lung cancer stem cells. *Drug Des. Dev. Ther.*, **2015**, *9*, 2399-2407. PMID: 25960639
- Montazi-Borojeni, A.A.; Abdollahi, E.; Ghasemi, F.; Caraglia, M.; Sahebkar, A. The novel role of pyrvinium in cancer therapy. *J. Cell. Physiol.*, **2018**, *233*(4), 2871-2881. <http://dx.doi.org/10.1002/jcp.26006> PMID: 28500633
- Deng, L.; Lei, Y.; Liu, R.; Li, J.; Yuan, K.; Li, Y.; Chen, Y.; Liu, Y.; Lu, Y.; Edwards, C.K., III; Huang, C.; Wei, Y. Pyrvinium targets autophagy addiction to promote cancer cell death. *Cell Death Dis.*, **2013**, *4*(5), e614. <http://dx.doi.org/10.1038/cddis.2013.142> PMID: 23640456
- Lamb, R.; Ozsvari, B.; Lisanti, C.L.; Tanowitz, H.B.; Howell, A.; Martinez-Outschoorn, U.E.; Sotgia, F.; Lisanti, M.P. Antibiotics that target mitochondria effectively eradicate cancer stem cells, across multiple tumor types: Treating cancer like an infectious disease. *Oncotarget*, **2015**, *6*(7), 4569-4584. <http://dx.doi.org/10.18632/oncotarget.3174> PMID: 25625193
- Tomitsuka, E.; Kita, K.; Esumi, H. The NADH-fumarate reductase system, a novel mitochondrial energy metabolism, is a new target for anticancer therapy in tumor microenvironments. *Ann. N. Y. Acad. Sci.*, **2010**, *1201*, 44-49. <http://dx.doi.org/10.1111/j.1749-6632.2010.05620.x> PMID: 20649538
- Thorne, C.A.; Hanson, A.J.; Schneider, J.; Tahinci, E.; Orton, D.; Cselenyi, C.S.; Jernigan, K.K.; Meyers, K.C.; Hang, B.I.; Waterson, A.G.; Kim, K.; Melancon, B.; Ghidoui, V.P.; Sulikowski, G.A.; LaFleur, B.; Salic, A.; Lee, L.A.; Miller, D.M., III; Lee, E. Small-molecule inhibition of Wnt signaling through activation of casein kinase 1 α . *Nat. Chem. Biol.*, **2010**, *6*(11), 829-836. <http://dx.doi.org/10.1038/nchembio.453> PMID: 20890287
- Ouelaa-Benslama, R.; Emami, S. Pinworm and TNKS inhibitors, an eccentric duo to derail the oncogenic WNT pathway. *Clin. Res. Hepatol. Gastroenterol.*, **2011**, *35*(8-9), 534-538. <http://dx.doi.org/10.1016/j.clinre.2011.03.015> PMID: 21782548

- [12] Carrella, D.; Manni, I.; Tumaini, B.; Dattilo, R.; Papaccio, F.; Mutarelli, M.; Sirci, F.; Amoreo, C.A.; Mottolose, M.; Iezzi, M.; Ciolli, L.; Aria, V.; Bosotti, R.; Isacchi, A.; Loreni, F.; Bardelli, A.; Avvedimento, V.E.; di Bernardo, D.; Cardone, L. Computational drugs repositioning identifies inhibitors of oncogenic PI3K/AKT/P70S6K-dependent pathways among FDA-approved compounds. *Oncotarget*, **2016**, *7*(37), 58743-58758. <http://dx.doi.org/10.18632/oncotarget.11318> PMID: 27542212
- [13] Esumi, H.; Lu, J.; Kurashima, Y.; Hanaoka, T. Antitumor activity of pyrvinium pamoate, 6-(dimethylamino)-2-[2-(2,5-dimethyl-1-phenyl-1H-pyrrol-3-yl)ethenyl]-1-methyl-quinolinium pamoate salt, showing preferential cytotoxicity during glucose starvation. *Cancer Sci.*, **2004**, *95*(8), 685-690. <http://dx.doi.org/10.1111/j.1349-7006.2004.tb03330.x> PMID: 15298733
- [14] Banerjee, A.; Jothimani, G.; Prasad, S.V.; Marotta, F.; Pathak, S. Targeting Wnt signaling through small molecules in governing stem cell fate and diseases. *Endocr. Metab. Immune Disord. Drug Targets*, **2019**, *19*(3), 233-246. <http://dx.doi.org/10.2174/1871530319666190118103907> PMID: 30657051
- [15] Nair, R.R.; Piktel, D.; Hathaway, Q.A.; Rellick, S.L.; Thomas, P.; Saralkar, P.; Martin, K.H.; Geldenhuys, W.J.; Hollander, J.M.; Gibson, L.F. Pyrvinium pamoate use in a b cell acute lymphoblastic leukemia model of the bone tumor microenvironment. *Pharm. Res.*, **2020**, *37*(3), 43. <http://dx.doi.org/10.1007/s11095-020-2767-4> PMID: 31989336
- [16] Smith, T.C.; Kinkel, A.W.; Gryczko, C.M.; Goulet, J.R. Absorption of pyrvinium pamoate. *Clin. Pharmacol. Ther.*, **1976**, *19*(6), 802-806. <http://dx.doi.org/10.1002/cpt1976196802> PMID: 1269218
- [17] Wiegering, A.; Uthe, F.W.; Hüttenrauch, M.; Mühling, B.; Linnebacher, M.; Krummenast, F.; Germer, C.T.; Thalheimer, A.; Otto, C. The impact of pyrvinium pamoate on colon cancer cell viability. *Int. J. Colorectal Dis.*, **2014**, *29*(10), 1189-1198. <http://dx.doi.org/10.1007/s00384-014-1975-y> PMID: 25060218
- [18] Lee, E.; Lee, L.; Thorne, C.; Tahinci, E.; Meyers, K.C. Pyrvinium for the treatment of cancer. US Patent 20,090,099,062A1, **2009**.
- [19] Mologni, L.; Brussolo, S.; Cecon, M.; Gambacorti-Passerini, C. Synergistic effects of combined Wnt/KRAS inhibition in colorectal cancer cells. *PLoS One*, **2012**, *7*(12), e51449. <http://dx.doi.org/10.1371/journal.pone.0051449> PMID: 23227266
- [20] Ye, Y.; Zhang, X.; Zhang, T. Design and evaluation of injectable niclosamide nanocrystals prepared by wet media milling technique. *Drug Dev. Ind. Pharm.*, **2015**, *41*(9), 1416-1424.
- [21] Gubernator, J. Active methods of drug loading into liposomes: Recent strategies for stable drug entrapment and increased *in vivo* activity. *Expert Opin. Drug Deliv.*, **2011**, *8*(5), 565-580. <http://dx.doi.org/10.1517/17425247.2011.566552> PMID: 21492058
- [22] Barenholz, Y. Relevancy of drug loading to liposomal formulation therapeutic efficacy. *J. Liposome Res.*, **2003**, *13*(1), 1-8. <http://dx.doi.org/10.1081/LPR-120017482> PMID: 12725720
- [23] Matbou Riahi, M.; Sahebkar, A.; Sadri, K.; Nikoofal-Sahlabadi, S.; Jaafari, M.R. Stable and sustained release liposomal formulations of celecoxib: *In vitro* and *in vivo* anti-tumor evaluation. *Int. J. Pharm.*, **2018**, *540*(1-2), 89-97. <http://dx.doi.org/10.1016/j.ijpharm.2018.01.039> PMID: 29371019
- [24] Alavizadeh, S.H.; Badiie, A.; Golmohammadzadeh, S.; Jaafari, M.R. The influence of phospholipid on the physicochemical properties and anti-tumor efficacy of liposomes encapsulating cisplatin in mice bearing C26 colon carcinoma. *Int. J. Pharm.*, **2014**, *473*(1-2), 326-333. <http://dx.doi.org/10.1016/j.ijpharm.2014.07.020> PMID: 25051111
- [25] Oku, N. Innovations in liposomal DDS technology and its application for the treatment of various diseases. *Biol. Pharm. Bull.*, **2017**, *40*(2), 119-127. <http://dx.doi.org/10.1248/bpb.b16-00857> PMID: 28154249
- [26] Xu, W.; Lacerda, L.; Debeb, B.G.; Atkinson, R.L.; Solley, T.N.; Li, L. The antihelminthic drug pyrvinium pamoate targets aggressive breast cancer. *PLoS One*, **2013**, *8*(8), e71508. <http://dx.doi.org/10.1371/journal.pone.0071508>
- [27] Ishii, I.; Harada, Y.; Kasahara, T. Reprofile a classical anthelmintic, pyrvinium pamoate, as an anti-cancer drug targeting mitochondrial respiration. *Front. Oncol.*, **2012**, *137*.
- [28] Yu, D.-H.; Macdonald, J.; Liu, G.; Lee, A.S.; Ly, M.; Davis, T. Pyrvinium targets the unfolded protein response to hypoglycemia and its anti-tumor activity is enhanced by combination therapy. *PLoS One*, **2008**, *3*(12), e3951. <http://dx.doi.org/10.1371/journal.pone.0003951>